

# Formation of nanosized Fe–Co alloys in $\alpha$ -Al<sub>2</sub>O<sub>3</sub> crystals by ion implantation

N. Hayashi<sup>a)</sup>

*Kurume Institute of Technology, 2228 Kamitsu-machi, Kurume-shi, Fukuoka 830-0052, Japan*

I. Sakamoto

*National Institute of Advanced Industrial Science and Technology, 1-1-1 Umezono, Tsukuba-shi, Ibaraki 305-8568, Japan*

H. Wakabayashi and T. Toriyama

*Musashi Institute of Technology, 1-28-1, Tamazutsumi, Setagaya-ku, Tokyo 158-8557, Japan*

S. Honda

*Shimane University, 1060 Nishikawatsu, Matsue-shi, Shimane 690-8504, Japan*

(Received 19 February 2003; accepted 27 May 2003)

Nanometer-sized Fe–Co composite clusters in  $\alpha$ -Al<sub>2</sub>O<sub>3</sub> matrices were synthesized by sequential implantation of Fe and Co ions with the projectiles' energy at 100 keV. The synthesized clusters were shown to have bcc structure by the measurement of glancing angle x-ray diffraction. We have observed an apparent change in the internal magnetic field of the Fe–Co composite clusters with changing Co concentration, which exhibits the maximum at a concentration around 25 at. % Co as revealed by conversion electron Mössbauer spectroscopy. The magnetoresistance ratio of the granules was observed to increase with the Co addition to the Fe nanoclusters. The results provide clear evidences on the alloy formation of Fe–Co nanoclusters in  $\alpha$ -Al<sub>2</sub>O<sub>3</sub> layers synthesized by ion implantation. © 2003 American Institute of Physics. [DOI: 10.1063/1.1592867]

## I. INTRODUCTION

Granular films formed by nanosized metal clusters embedded in oxide matrices are known to exhibit peculiar magnetic properties, offering valuable applications in material science and the development of preparation methods for the metal-ceramic oxides composites.<sup>1,2</sup> Nanosized metal clusters have been synthesized within the matrices by various techniques including the use of ion beams.<sup>1</sup> We have found that the surface layer of  $\alpha$ -Al<sub>2</sub>O<sub>3</sub> crystals implanted with Fe ions to a dose of  $1.0 \times 10^{17}$  ions/cm<sup>2</sup> shows tunneling-type giant magnetoresistance (TMR) property,<sup>3</sup> and the magnetoresistance (MR) ratio obtained was nearly twice as large as that in Fe–Al–O granular thin films prepared by sputtering.<sup>4</sup> It has been concluded that the precipitation of implanted irons as superparamagnetic clusters is responsible for the large TMR. In our further study the dose dependence of the TMR effects was investigated in the Fe/Al<sub>2</sub>O<sub>3</sub> granules and the highest MR ratio was observed at the dose around  $1.5 \times 10^{17}$  ions/cm<sup>2</sup> where the blocking of superparamagnetic relaxation starts at room temperature in the iron granules.<sup>5</sup> Furthermore, we have suggested the possibility that sequentially implanted Fe and Co ions are aggregated into clusters in the Al<sub>2</sub>O<sub>3</sub> matrices leading to the formation of Fe–Co granules,<sup>6</sup> but it remains uncertain whether they are mixed into alloy clusters and in what manner the magnetic properties changes in the formed granular layers.

In this article we report the magnetic properties of Fe–Co alloy nanoclusters prepared by the sequential implantation of Fe and Co ions. It is observed that the internal magnetic fields  $B_{\text{hf}}$  plotted against Co concentration exhibit a curve quite similar to the well-known Slater–Pauling's curve for the magnetism of transition metal alloys. The results provide evidence on the formation of Fe–Co alloy clusters in the granular layers synthesized by ion implantation.

## II. EXPERIMENT

Sequential implantations of <sup>57</sup>Fe ions followed by <sup>59</sup>Co ions were performed at room temperature at two doses of  $1.5 \times 10^{17}$  and  $2.0 \times 10^{17}$  ions/cm<sup>2</sup> with the projectiles' energy of 100 keV and a beam flux of about  $2 \mu\text{A}/\text{cm}^2$  into high purity single-crystalline samples of  $\alpha$ -Al<sub>2</sub>O<sub>3</sub> with *R*-cut plane tilted 5° with respect to the ion beam. The projected range of the implanted ions was estimated as 50 nm by TRIM code. The atomic concentrations of Fe–Co composites were denoted by the relative amount of implanted doses for the two kinds of magnetic ions. For example, the doses were  $1.13 \times 10^{17}$  Fe/cm<sup>2</sup> and then  $0.37 \times 10^{17}$  Co/cm<sup>2</sup> for the case of  $1.50 \times 10^{17}$  (Fe+Co)/cm<sup>2</sup> with 25 at. % Co. At a dose of  $2.0 \times 10^{17}$  ions/cm<sup>2</sup> the relative amount of the two magnetic ions was varied to investigate the concentration dependence of the hyperfine parameters. The crystallinity of the implanted layers was characterized by glancing angle x-ray diffraction (GXR). The GXR patterns were measured with a glancing angle of  $\theta = 3.5^\circ$ , using Cu targets. The internal fields were measured by conversion electron Mössbauer spectroscopy (CEMS). CEMS was taken with a He

<sup>a)</sup> Author to whom correspondence should be addressed; electronic mail: nhayashi@cc.kurume-it.ac.jp

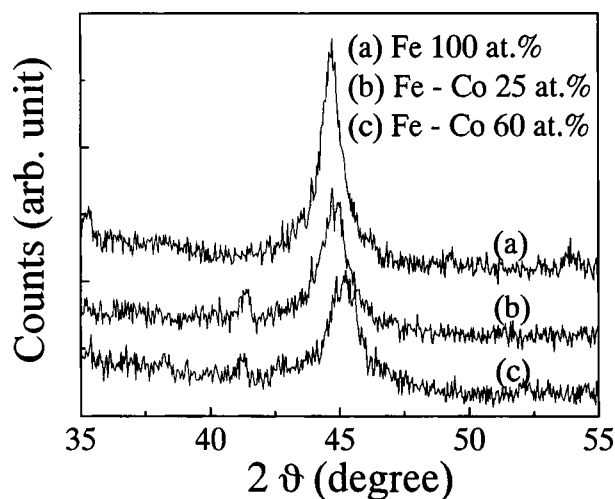


FIG. 1. GXR D patterns in Fe-Co composites in  $\alpha$ - $\text{Al}_2\text{O}_3$  matrices with Co concentration of 0% (upper curve), 25 at. % (middle curve), and 60 at. % (lower curve), obtained by sequential implantation to a total dose of  $2.0 \times 10^{17}$  ions/cm<sup>2</sup>.

–4%  $\text{CH}_4$  gas flow proportional counter in which the sample was placed in backscattering geometry, using a 740 MBq  $^{57}\text{Co}$  source in Rh matrix. Mössbauer spectra were analyzed by least-squares fitting with overlapping Lorentzian curves to obtain the parameters of hyperfine interaction. The MR of the implanted Fe-Co/ $\text{Al}_2\text{O}_3$  granules was measured using a dc method. The implantations and all measurements were performed at room temperature.

### III. RESULTS AND DISCUSSION

Cobalt is known to form a continuous range of solid solutions with iron, whose structures at room temperature are bcc for 0–73 at. % Co and fcc for 73–92% Co.<sup>7</sup> Figure 1 shows typical GXR D pattern of Fe and Fe-Co granular layers after implantation to a total dose of  $2.0 \times 10^{17}$  ions/cm<sup>2</sup> with Fe and/or Co ions. A rather sharp peak appears at  $2\theta = 44^\circ - 46^\circ$  corresponding to the diffraction from the bcc  $\alpha$ -Fe (110) planes. The GXR D peaks were analyzed by the least-squares fitting assuming Gaussian curves, and the obtained lattice parameters are summarized in Table I. While the lattice parameter obtained as 0.287 nm for the Fe granules is in agreement with bulk  $\alpha$ -iron, the decrease in the parameters with increasing Co concentration is also consistent with the change in the bulk Fe-Co alloys, as referred to 1997 JCPDS-International Center for Diffraction Data. The results confirm that Fe-based alloy clusters with bcc phase are formed in the implanted layers. Furthermore, the granule

TABLE I. X-ray diffraction data and lattice parameters of the Fe-Co/ $\text{Al}_2\text{O}_3$  granular samples prepared by Fe and Co implantation to a total dose of  $2.0 \times 10^{17}$  ions/cm<sup>2</sup>

Granules	$2\theta$	Peak width	Lattice parameter (nm)	Granules' diameter (nm)
Fe (100%)	44.68°	1.15°	0.287	7.5
Fe-Co (25%)	44.79°	1.38°	0.286	6.2
Fe-Co (60%)	45.16°	1.45°	0.284	5.9

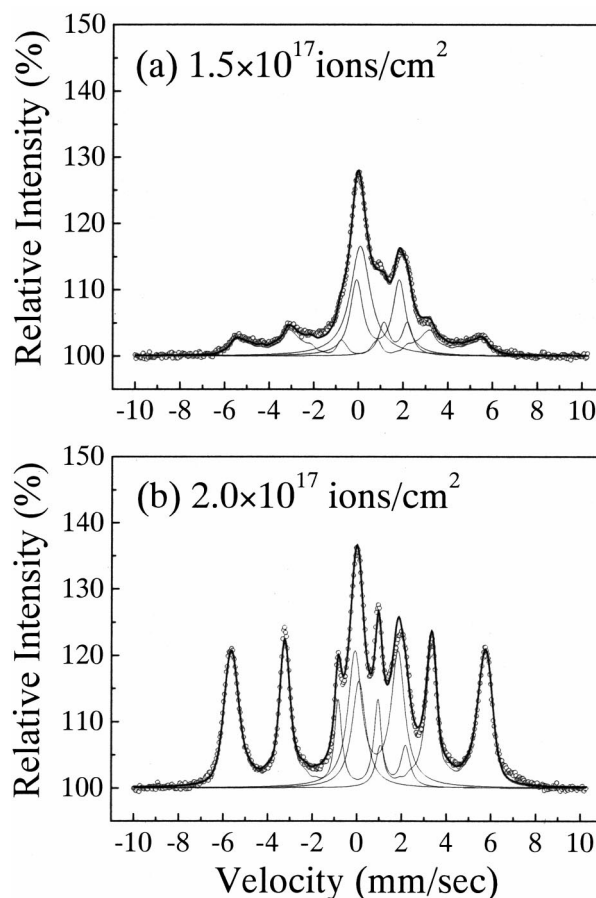


FIG. 2. CEMS spectra taken from Fe-Co composites in  $\alpha$ - $\text{Al}_2\text{O}_3$  matrices with 25 at. % Co obtained by sequential implantation of Fe and Co ions to total doses of  $1.5 \times 10^{17}$  ions/cm<sup>2</sup> (a) and  $2.0 \times 10^{17}$  ions/cm<sup>2</sup> (b).

sizes listed in Table I supplement the estimation obtained by the analysis of CEMS spectra, which were measured with applying magnetic fields, because the sizes in Fe clusters have been reported to distribute around two diameters of 3.5 and 6.2 nm in  $\text{Al}_2\text{O}_3$  matrix with an implantation dose of  $1.5 \times 10^{17}$  Fe/cm<sup>2</sup>.<sup>8</sup> It is noted that the CEMS analysis is based on the fact that the superparamagnetic particles present the evolution of magnetically split lines in CEMS due to the blocking of the magnetic relaxation under the applied magnetic field.

Figure 2 shows the CEMS spectra taken from the samples with total doses of  $1.5 \times 10^{17}$  ions/cm<sup>2</sup> and  $2.0 \times 10^{17}$  ions/cm<sup>2</sup> where the relative dose of Co ions to the total dose (Fe+Co) was kept to be 25%. The CEMS spectra were analyzed under the assumption that the spectra consist of a magnetic sextet, one single line, and two quadrupole doublets. A single line component located near zero velocity has been confirmed to arise from the superparamagnetic  $\alpha$ -Fe clusters<sup>5,8</sup> and is referred to as the  $\text{Fe}^0$  state. Two doublets are assigned to two forms of the ferrous irons ( $\text{Fe}_{1,2}^{2+}$ ), which are supposed to arise from iron oxides in the complex form.<sup>9</sup> A distribution in the internal fields  $B_{\text{hf}}$  was assumed for the analysis of the broad sextet lines. Of the two samples it appears that the CEMS pattern with a dose of  $1.5 \times 10^{17}$  ions/cm<sup>2</sup> indicates a broader  $B_{\text{hf}}$  distribution, which seems to manifest wider distribution in the sizes of nanoclus-

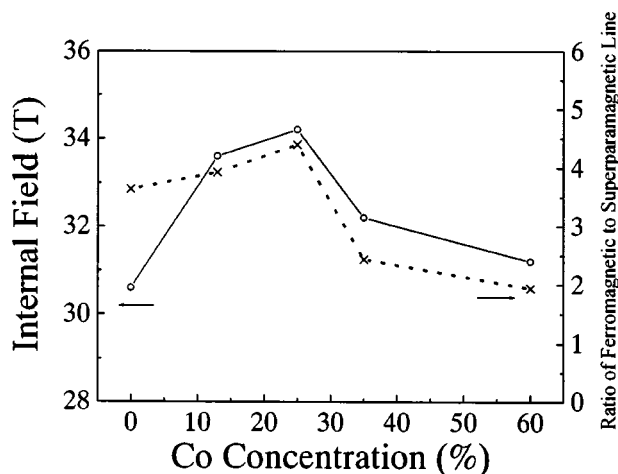


FIG. 3. Concentration dependence of the averaged internal field  $B_{\text{hf}}$  at iron sites (solid curve) and the intensity ratio of the ferromagnetic FM lines to the superparamagnetic SP one (broken curve) plotted against Co concentration. The total dose of the Fe and Co implantation is  $2.0 \times 10^{17}$  ions/cm<sup>2</sup>.

ters. When increasing the dose to  $2.0 \times 10^{17}$  ions/cm<sup>2</sup>, the ferromagnetic (FM) lines increase in intensity at the expense of the superparamagnetic (SP) Fe<sup>0</sup> line and at the same time exhibit sharper line shapes. The relative intensity ratio FM/SP increases from 0.86 to 4.4 with increasing the total doses from  $1.5 \times 10^{17}$  to  $2.0 \times 10^{17}$  ions/cm<sup>2</sup>. The increase in the FM/SP ratio indicates that during the dose increment by  $0.5 \times 10^{17}$  ions/cm<sup>2</sup> the superparamagnetic relaxation is effectively blocked at room temperature in the Fe–Co nanoclusters with 25 at. % Co. The start of the blocking at these dose range is in good agreement with the observation in Fe/Al<sub>2</sub>O<sub>3</sub> granules without Co ions.<sup>5</sup> Furthermore, the magnetic sextet in Fig. 2(a) appears with the peak positions corresponding to  $B_{\text{hf}} = 33.8$  T. The results suggest that Co ions contribute not only to the growth of the iron clusters formed by precedently implanted <sup>57</sup>Fe ions but also to alloying the irons because the  $B_{\text{hf}}$  value is larger than the value of 33.0 T in bulk  $\alpha$ -iron. It should be noted that we monitor the growth of the nanoclusters just by the <sup>57</sup>Fe in the sequential implantation.

CEMS spectra were measured with changing the relative Fe–Co concentration from 0 to 60 at. % at a total dose of  $2.0 \times 10^{17}$  ions/cm<sup>2</sup>. The best fitting of CEM spectra for the samples prepared by sequential implantation of Fe and Co ions was obtained with the isomer values of 0.04–0.05 mm/s for the FM lines, slightly larger than that of Fe implanted Al<sub>2</sub>O<sub>3</sub> granules (less than 0.01 mm/s). The values of the isomer shift at iron sites are in good agreement with those in bulk Fe–Co alloys observed by Vincze *et al.*,<sup>10</sup> indicating an increase in the number of iron *d* electrons. Figure 3 shows the averaged value of  $B_{\text{hf}}$  as a function of Co concentration, together with the relative intensity ratio of FM to SP lines. Remarkably, the maximum value of  $B_{\text{hf}}$  is achieved at Co concentrations near 25 at. %. Many studies have been published on the concentration dependence of the average internal field at iron sites in bulk Fe–Co alloys,<sup>7,10</sup> and the maximum  $B_{\text{hf}}$  value has been reported to be 36.5 T at the Co concentration of 30 at. % while the average  $B_{\text{hf}}$  in the nano-

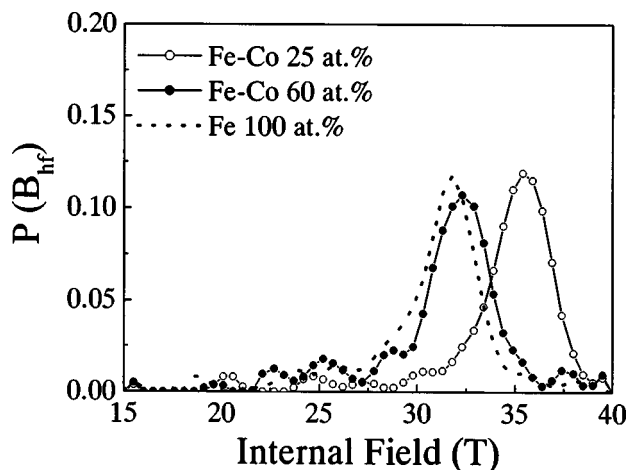


FIG. 4. Distribution of  $B_{\text{hf}}$  in Fe–Co clusters with the Co concentration of 0, 25, and 60 at. % at the total doses of  $2.0 \times 10^{17}$  ions/cm<sup>2</sup>, obtained from the analyses of CEMS spectra.

clusters with 25 at. % Co has been observed to be 34.2 T in Fig. 3. It should be noted that the  $B_{\text{hf}}$  value cited in our previous report<sup>6</sup> denotes the peak values in the  $B_{\text{hf}}$  distribution, which is higher than the average  $B_{\text{hf}}$  value due to the asymmetry of the  $B_{\text{hf}}$  distribution as shown in Fig. 4. The reduction of the average value observed for the Fe–Co nanoclusters, compared to those in bulk Fe–Co alloys, can be explained by the influence of collective magnetic excitations.<sup>11</sup> The difference of the concentration dependence between the nanoclusters and the bulk alloys is likely to be caused by the particular behavior of the transition from the superparamagnetic to the ferromagnetic state at the lower Co concentration as can be seen in the plots of FM/SP intensity ratio, which is to be discussed later. However, it is significant that the variation of  $B_{\text{hf}}$  with Co concentration in the nanoclusters shows similar characteristics to the variation of saturation magnetic moment for the alloys of the first transition group metals, plotted as a function of the electron concentration.

The empirical relation between  $B_{\text{hf}}$  and the atomic moment is given by the expression

$$B_{\text{hf}} = a \cdot \mu(\text{Fe}) + b \cdot \mu',$$

where  $\mu(\text{Fe})$  is the magnetic moment of Fe atom,  $\mu'$  is the average magnetic moment of the alloy, and *a* and *b* are proportionality constants.<sup>10</sup> Using the constants empirically determined by Vincze, *i.e.*,  $a = 7.0 \text{ T}/\mu_B$  and  $b = (8.0 - 3.3 c_{\text{Co}}) \text{ T}/\mu_B$ , we obtain  $\mu(\text{Fe}) = 2.4 \mu_B$  for the  $B_{\text{hf}}$  value of 34.2 T observed at the concentration of 25 at. % Co, *i.e.*,  $c_{\text{Co}} = 0.25$ . Figure 4 shows typical distribution curves of  $B_{\text{hf}}$  in the Fe–Co clusters with three Co concentrations of 0, 25, and 60 at. %. We do not notice any essential differences in the characteristics of these distribution curves, *i.e.*, they have a similar full width at half maximum. Therefore, the nanoclusters appear to have a rather sharp  $B_{\text{hf}}$  distribution and the average value is well defined regardless of the Co contents. The both results of the sharp distribution and increase in  $B_{\text{hf}}$  with mixing Fe clusters with Co indicate that the implanted Fe and Co ions are uniformly distributed within the nano-

composite clusters, and the intimate interactions between the Fe and the Co atoms are comparable to that in bulk Fe–Co alloys. It should be noted that the peak value in the  $B_{\text{hf}}$  distribution is 35.5 T, which is close to the maximum  $B_{\text{hf}}$  of 36.5 T observed in bulk Fe–Co alloys, and that the  $B_{\text{hf}}$  distribution in the nanoclusters extends to over 37.5 T.

The superparamagnetic relaxation time  $\tau$  in nanoclusters can be expressed as

$$\tau = \tau_0 \cdot \exp(KV/kT)$$

where  $K$  is the anisotropy constant and  $V$  the volume of the clusters. The prefactor  $\tau_0$  is typically of the order of  $10^{-10}$ – $10^{-12}$  s.<sup>11</sup> This equation shows that the growth of the cluster volume due to the increase of total (Fe+Co) dose leads to a longer relaxation time and likewise the transition from superparamagnetism to ferromagnetism. This has been observed to occur mainly at the total dose range of  $(1.5 - 2.0) \times 10^{17}$  ions/cm<sup>2</sup>. At  $2.0 \times 10^{17}$  ions/cm<sup>2</sup> with 25 at. % Co the intensities of FM and SP lines relative to the total spectral areas are measured to be 55.8% and 12.7%, respectively, i.e., FM/SP=4.4, as mentioned before. In Fig. 3 the extent of the transition is exhibited by the area intensity ratio, FM/SP. The plots manifest a concentration dependence similar to that of  $B_{\text{hf}}$ , indicating that it follows the change in magnetic moment of atom, except near the concentration of 0 at. % Co, i.e., pure iron. As the anisotropy constant is another parameter to determine the superparamagnetic relaxation time, the result suggests that the Co addition in the iron clusters causes a change in magnetic anisotropy energy. It has been reported by the work of Hall<sup>12</sup> that the first anisotropy constant is lowered with the Co addition in the Fe–Co alloy.

It is quite safe to conclude from the earlier results that sequential implantation of Fe and Co ions into  $\alpha$ -Al<sub>2</sub>O<sub>3</sub> matrix at room temperature leads to alloy formation of Fe–Co nanoclusters in the as-implanted conditions, i.e., without postannealing. Ferromagnetic clusters distributed in an insulator matrix are expected to form granular materials with tunneling-type magnetoresistance. Our results suggest that improvement in TMR characteristics, i.e., higher MR ratio, can be achieved in the granules by alloying Fe–Co clusters, because the resistivity change with external field is known to be proportional to the square of the magnetization in the granular layers.<sup>13</sup> The MR ratio is defined by

$$-\Delta\rho(H)/\rho(0) = -[\rho(H) - \rho(0)]/\rho(0),$$

where  $\rho(H)$  and  $\rho(0)$  are the resistivities at an external field  $H$  and 0 T, respectively. We have reported that the highest MR ratio in iron granules is 7.5% for external magnetic field of  $H = 1.2$  T at a dose of  $1.5 \times 10^{17}$  ions/cm<sup>2</sup>.<sup>4</sup> Figure 5 presents MR curves in Fe–Co granules for doses of  $1.5 \times 10^{17}$  ions/cm<sup>2</sup> with Co concentrations of 25 and 33 at. %, measured with external fields  $H$  parallel to the sample face, i.e., to the implantation layers. It is demonstrated that Fe–Co alloying improves the TMR characteristics; for example, the addition of 25 at. % Co results in 20% higher MR ratio than that for the granules without Co. Although we cannot ascertain that the magnetic layers synthesized by ion implantation has the best characteristics in TMR effect, MR ratio obtained

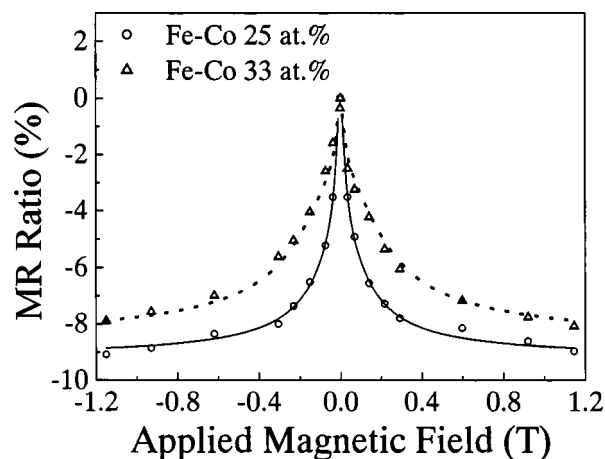


FIG. 5. Field dependence of room temperature MR curves of Fe–Co/Al<sub>2</sub>O<sub>3</sub> granules with 25 at. % Co (solid line) and 33 at. % Co (dotted line), prepared by sequential implantation of Fe and Co ions to the doses of  $1.5 \times 10^{17}$  ions/cm<sup>2</sup>.

in Fig. 5 is to date one of the best among the Fe–Co and Fe–Al–O granular films prepared by sputter deposition.<sup>4,14</sup>

Ion implantation has been established as one of the techniques to form bulk alloys, but only a few works have been done to synthesize nanosized alloy clusters with well-defined magnetic characteristics. Although Fe–Co nanoparticles were formed by techniques such as arc-discharge synthesis,<sup>15</sup> these nanoparticles have significant varieties in the phase structure and magnetic properties, depending on the preparation conditions such as evaporating and subsequent quenching. Some works have been published on the formation of binary alloy-based nanocomposites such as Ni–Co using ion beams and postannealing, but it was rather difficult to obtain clear evidence on alloying, because the available information is still limited for extremely small particles owing to their magnetic relaxations.<sup>16</sup> On the other hand, it is noteworthy that our granules offer the superior nanocomposite system to investigate the magnetic properties such as the extraordinary magnetic moments which can be evolved only in particles with low dimension.<sup>17</sup> It can be inferred from the  $B_{\text{hf}}$  distribution that the internal magnetic fields in our nanoparticles exceeds those in the bulk alloys.

#### IV. CONCLUSION

Our study has provided clear evidence of Fe–Co alloying in nanocomposites by the sequential implantation of Fe and Co ions, demonstrating the increase in the magnetic moment of Fe atom. It is remarkable that even in the as-implanted condition the Co ions are effectively and homogeneously mixed into the iron clusters formed prior to the Co implantation, leading to the formation of Fe–Co alloys with well-defined magnetic characteristics. In the case of iron based alloy CEMS combined with the mass selected <sup>57</sup>Fe implantation has been demonstrated to be useful in investigating the alloying process and magnetism in nanosized particles. The results offer the possibility of forming the variety of alloy nanoclusters and nanocomposite granules useful for the TMR applications.

**ACKNOWLEDGMENTS**

A part of this study was financially supported by the Budget for Nuclear Research of the Ministry of Education, Culture, Sports, Science and Technology, based on the screening and counseling by the Atomic Energy Commission.

- <sup>1</sup>G. L. Zhang and H. Pattyn, *Hyperfine Interact.* **113**, 165 (1998).  
<sup>2</sup>M. Murayama, J. M. Howe, H. Hidaka, and S. Takaki, *Science* **295**, 2433 (2002).  
<sup>3</sup>I. Sakamoto, S. Honda, H. Tanoue, N. Hayashi, and H. Yamane, *Nucl. Instrum. Methods Phys. Res. B* **148**, 1039 (1999).  
<sup>4</sup>S. Mitani, Y. Shintani, S. Ohnuma, and H. Fujimori, *J. Magn. Soc. Jpn.* **21**, 465 (1997).  
<sup>5</sup>N. Hayashi, T. Toriyama, H. Tanoue, H. Wakabayashi, and I. Sakamoto, *Hyperfine Interact.* **141/142**, 163 (2002).  
<sup>6</sup>N. Hayashi, T. Toriyama, H. Wakabayashi, I. Sakamoto, T. Okada, and

- K. Kuriyam, *Surf. Coat. Technol.* **158/159**, 193 (2002).  
<sup>7</sup>C. E. Johnson, M. S. Ridout, and T. E. Granshaw, *Proc. Phys. Soc.* **81**, 1079 (1963).  
<sup>8</sup>H. Wakabayashi, T. Hirai, T. Toriyama, N. Hayashi, and I. Sakamoto, *Phys. Status Solidi A* **189**, 515 (2002).  
<sup>9</sup>C. J. McHargue, P. S. Sklad, C. W. White, G. C. Farlow, A. Perez, and G. Marest, *J. Mater. Res.* **6**, 2145 (1991).  
<sup>10</sup>I. Vincze, I. A. Campbell, and A. J. Meyer, *Solid State Commun.* **15**, 1495 (1974).  
<sup>11</sup>F. Bødker and S. Mørup, *Hyperfine Interact.* **93**, 1421 (1994).  
<sup>12</sup>R. C. Hall, *J. Appl. Phys.* **31**, 157S (1960).  
<sup>13</sup>S. Honda, M. Nawate, M. Tanaka, and T. Okada, *J. Appl. Phys.* **82**, 764 (1997).  
<sup>14</sup>S. Mitani, H. Fujimori, and S. Ohnuma, *J. Magn. Magn. Mater.* **165**, 141 (1997).  
<sup>15</sup>X. L. Dong, Z. D. Zhang, S. R. Jin, and B. K. Kim, *J. Magn. Magn. Mater.* **210**, 143 (2000).  
<sup>16</sup>F. Gonella, *Nucl. Instrum. Methods Phys. Res. B* **166/167**, 831 (2000).  
<sup>17</sup>S. N. Khanna and S. Linderoth, *Phys. Rev. Lett.* **67**, 742 (1991).